

## FIBRINOGEN ADSORPTION ONTO BIOGLASS ALUMINOSILICATES

SIMONA CAVALU\*, VIORICA SIMON\*\*, F. BĂNICĂ\*, C. DELEANU\*\*\*

\* Faculty of Medicine and Pharmacy, University of Oradea, 10, P-ța 1 Decembrie,  
Oradea, Romania [scavalu@rdslink.ro](mailto:scavalu@rdslink.ro)

\*\*Faculty of Physics, "Babeș-Bolyai" University, 1, Kogălniceanu St., Cluj-Napoca, Romania

\*\*\*Institute of Organic Chemistry, 202-B, Splaiul Independenței, Bucharest, Romania

*Abstract.* Sol-gel method was chosen in order to prepare different aluminosilicate materials. This study is focused on FTIR spectroscopy and differential thermal analysis of  $\text{Al}_2\text{O}_3$ - $\text{SiO}_2$  binary system, followed by Simulated Body Fluid investigation as bioactivity evidence. The biocompatibility of the samples was evaluated with respect to fibrinogen adsorption using ATR FTIR technique. Deconvolution of amide I band of fibrinogen upon adsorption indicates that aluminosilicates prepared with silicic acid as starting material exhibit a superior biocompatibility compared with that of the sample obtained with TEOS.

*Key words:* Aluminosilicate, fibrinogen, FTIR.

### INTRODUCTION

Protein adsorption onto medical implants is an essential aspect of the cascade of biological reactions taking place at the interface between the synthetic material and biological environment. The type and amounts of adsorbed proteins mediate subsequent adhesion, proliferation and differentiation of cells as well as depositing of mineral phase. Biocompatibility is dictated by the manner in which the biomaterial surfaces interact with blood constituents (erythrocytes, platelets) as well as with proteins. The behavior of a protein at an interface is likely to differ considerably from its behavior in the bulk. Because of the different local environment at the interface, the protein may have the opportunity of adopting a more disordered state exposing its hydrophobic core to the aqueous phase, often called surface denaturation. The denaturation of secondary structure involves also

---

Received: May 2007;  
in final form September 2007.

ROMANIAN J. BIOPHYS., Vol. 17, No. 4, P. 237–245, BUCHAREST, 2007

changes in ratio among the three common structures:  $\alpha$  helix,  $\beta$  sheets or turns and unordered. The spectral regions of amide I ( $1660\text{ cm}^{-1}$ ), amide II ( $1550\text{ cm}^{-1}$ ) and amide III ( $1300\text{ cm}^{-1}$ ) are very sensitive to the conformational changes in the secondary structure of proteins. ATR-FTIR spectroscopy has a sufficient sensitivity to examine the structure of proteins in solution or adsorbed on different surfaces [1, 10]. Computational techniques based on the second derivative spectra and deconvolution procedure is used for percentage evaluation of each secondary structure and also the perturbations upon the adsorption to different surfaces.

Plasma fibrinogen is one of the most relevant proteins that are adsorbed on biomaterial surfaces because it takes part in blood coagulation, facilitates adhesion and aggregation of platelets, which are very important properties in the processes of both haemostasis and thrombosis. It is a 340 kDa dimeric protein and the model comprised three spherical regions connected by two narrow rods. According to the current view [4], the protein has two sets of three non-identical polypeptide chains ( $\alpha$ ,  $\beta$  and  $\gamma$ ), held together by 29 disulfide bonds. The molecular length of fibrinogen is 47.5 nm, with a diameter of the roughly spherical D and E domains of 6.5 and 5 nm, respectively. Each connector region is 0.8–1.5 nm in diameter and 16 nm in length (Fig.1).

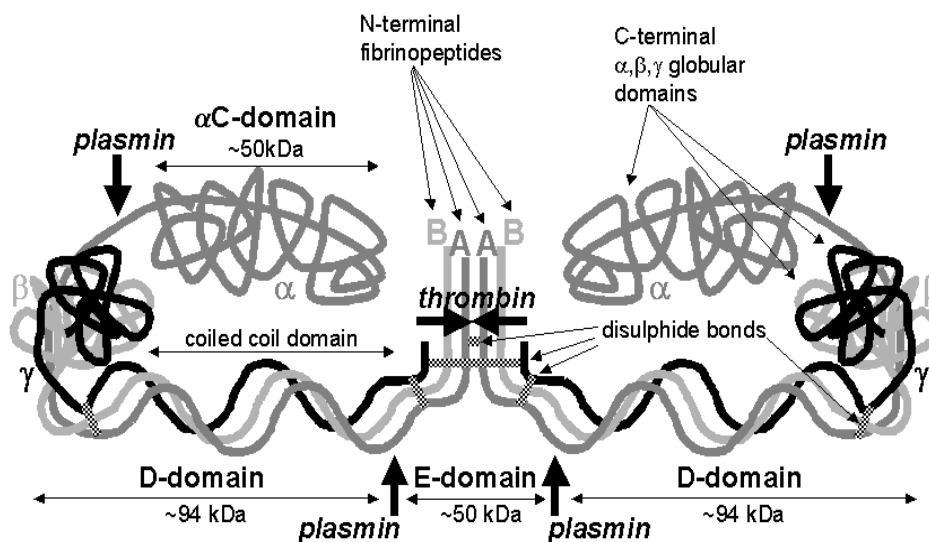


Fig.1. Tertiary structure of fibrinogen, consisting of two sets of non-identical peptide chains.

The aim of our study is to investigate the behavior of fibrinogen adsorbed onto different aluminosilicate bioglass matrices used in radiotherapy and hyperthermia.

## EXPERIMENTAL

Fibrinogen fraction I type IV from pig plasma was obtained from SIGMA. Reagent-grade tetraethylorthosilicate (TEOS,  $\text{Si}(\text{OC}_2\text{H}_5)_4$ ) or silicic acid ( $\text{SiO}_x(\text{OH})_{4-2x}$ ) and aluminum nitrate  $\text{Al}(\text{NO}_3)_3 \cdot 9\text{H}_2\text{O}$  were used as starting materials to prepare, by a sol-gel process, aluminosilicate samples ( $\text{Al}_2\text{O}_3 \cdot 2\text{SiO}_2$ ). White powder samples were characterized using thermal and infrared spectroscopic analyses. Infrared spectroscopic analysis was carried out also on samples heat treated in air at  $950^\circ\text{C}$ , under normal pressure. Powder samples were incubated for 24 hours at  $37^\circ\text{C}$  in 2 mg/ml protein phosphate buffered solution and, after filtration and drying process, the surfaces were analyzed by ATR FTIR spectroscopy. The FT-IR spectra of samples before and after incubation were recorded in the region  $4000\text{--}800\text{ cm}^{-1}$  by a Bruker EQUINOX 55 spectrometer OPUS software, using an Attenuated Total Reflectance accessory and KBr technique as well. The second derivative spectral analysis was applied to locate positions and assign them to different functional groups of adsorbed protein, baseline-corrected using the method of Dong and Caughey [8], and area-normalized under the second derivative amide I region,  $1700\text{--}1600\text{ cm}^{-1}$ . Curve fitting was performed by setting the number of component bands found by second-derivative analysis with fixed bandwidth ( $12\text{ cm}^{-1}$ ) and Gaussian profile.

## RESULTS AND DISCUSSION

Prior to the adsorption properties investigation of the aluminosilicate samples, the structural properties were characterized using thermal and infrared spectroscopic analyses. Differential thermal analysis results were already pointed out [7] emphasizing that removal of free water takes place at a significantly lower temperature for the aluminosilicate samples prepared with silicic acid, as compared with similar samples with TEOS.

FTIR analysis using KBr disk technique shows spectroscopic changes for  $\text{Al}_2\text{O}_3 \cdot 2\text{SiO}_2$  samples when they are prepared with silicic acid or TEOS as silicon source (Fig. 2). The presence of water is indicated by the broad bands at  $3400$ ,  $3100$  and  $1640\text{ cm}^{-1}$  the latest being connected with the bending vibrations of the H-OH bond from adsorbed water.

The  $1380\text{ cm}^{-1}$  band is assigned to N-O stretching vibration and indicates the presence of  $\text{NO}_3^-$  species resulting from thermal decomposition of aluminum nitrate. Other nitrogen species also occur as reflected by the larger band centered at  $1400\text{ cm}^{-1}$ [2]. The intensity of this band is much higher in the case of using TEOS

(Fig. 2b). The bands located at  $470\text{ cm}^{-1}$  in Fig. 2a and the corresponding band at  $440\text{ cm}^{-1}$  in Fig. 2b are related to the bending vibrations of Si-O-Si bonds, while the large bands around  $1100\text{ cm}^{-1}$  are assigned to stretching vibration of Si-O-Si and Al-O-Al bonds. The correlation between IR absorption bands and different types of aluminate polyhedra is based on IR results obtained for aluminate crystals [6, 11]. The Al-O stretching vibrations of tetrahedral  $\text{AlO}_4$  groups are related with the bands in the region  $900\text{--}750\text{ cm}^{-1}$ , while the bands in the region  $650\text{--}500\text{ cm}^{-1}$  are associated with stretching modes of  $\text{AlO}_6$  octahedra. In the case of our samples, the band at  $570\text{ cm}^{-1}$  is assigned to Al-O vibrations in  $\text{AlO}_6$  and that at  $800\text{ cm}^{-1}$  to  $\text{AlO}_4$  units. As observed in Fig. 2, the corresponding bands of silicium and aluminum structural units are shifted to lower wavenumbers for the samples prepared with TEOS, showing a much stiff and disordered network for this sample. In Fig. 3 are displayed the FTIR spectra of the  $\text{Al}_2\text{O}_3\cdot 2\text{SiO}_2$  sol-gel samples with silicic acid before and after their thermal treatment at  $950^\circ\text{C}$ . The applied heat treatment does not lead to sample crystallisation because neither new absorption bands nor a peak narrowing occurs. The main change is the almost complete disappearance of the band typical to nitrogen species around  $1400\text{ cm}^{-1}$ . Similar results are obtained also for the samples prepared with TEOS.

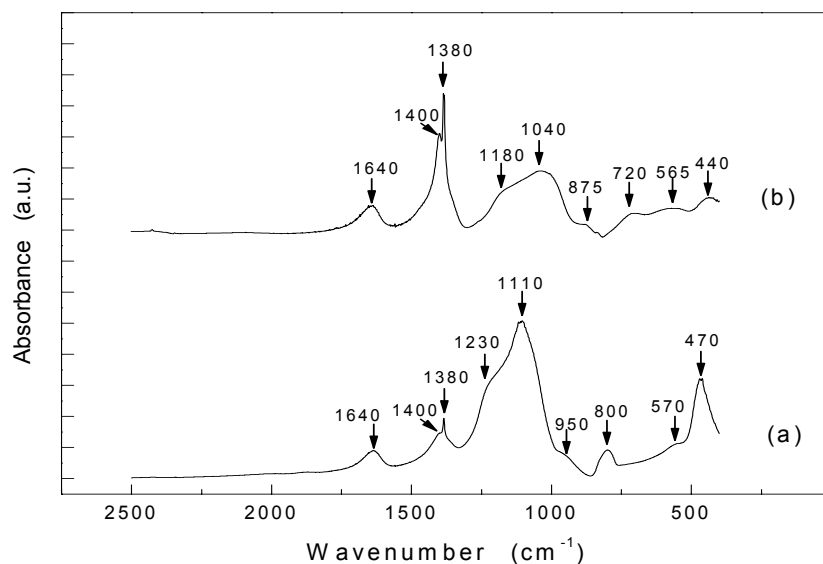


Fig. 2. FTIR spectra (KBr disk technique) recorded from  $\text{Al}_2\text{O}_3\cdot 2\text{SiO}_2$  sol-gel samples prepared with silicic acid (a) and TEOS (b).

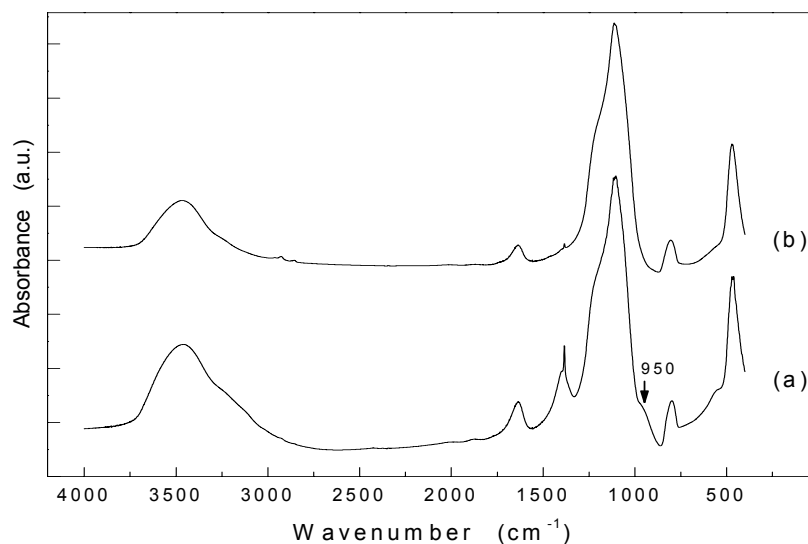


Fig. 3. FTIR spectra of  $\text{Al}_2\text{O}_3 \cdot 2\text{SiO}_2$  sol-gel samples with silicic acid as prepared (a) and heat treated at  $950^\circ\text{C}$  (b).

As our aim is to study the surfaces properties of the materials, ATR FTIR technique is applied for both aluminosilicates before and after incubation for 24 h at  $37^\circ\text{C}$ . ATR FTIR spectrum of fibrinogen, as received from Sigma Chemicals, is displayed in Fig. 4, emphasizing the amide dominant bands.

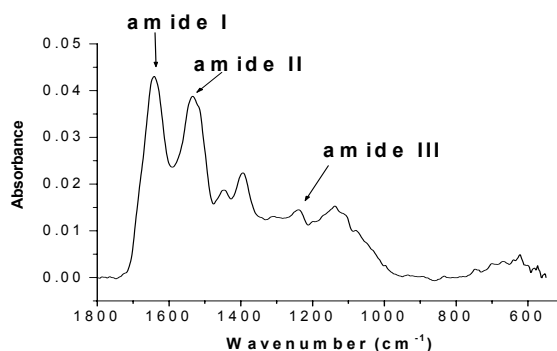


Fig. 4. ATR FTIR spectrum of fibrinogen type IV from pig plasma.

The amide I band, located between  $1700$  and  $1600\text{ cm}^{-1}$  is composed mainly (around 80%) of the  $\text{C}=\text{O}$  stretching vibration of the peptidic bond, while amide II vibrations derives mainly from in plane  $\text{N-H}$  bending (40–60%),  $\text{C-N}$  (18–40%) and  $\text{C-C}$  (10%) stretching vibrations located between  $1530$ – $1560\text{ cm}^{-1}$ . Amide III

(between 1220 and 1320  $\text{cm}^{-1}$ ) is a more complex vibrational mode. This is mainly the in-phase combination of NH in-plane-bending and CN stretching with contributions from CC stretching and CO in-plane-bending, depending on the details of the force field, the nature of side chains and hydrogen bonding. Fig. 5a, b presents the ATR FTIR spectra of the sample prepared with silicic acid in the range 1800–600  $\text{cm}^{-1}$ , before (a) and after 24 h incubation (b) in fibrinogen solution 2 mg/ml. The corresponding spectra of the sample prepared with TEOS are displayed in Fig. 5c, d.

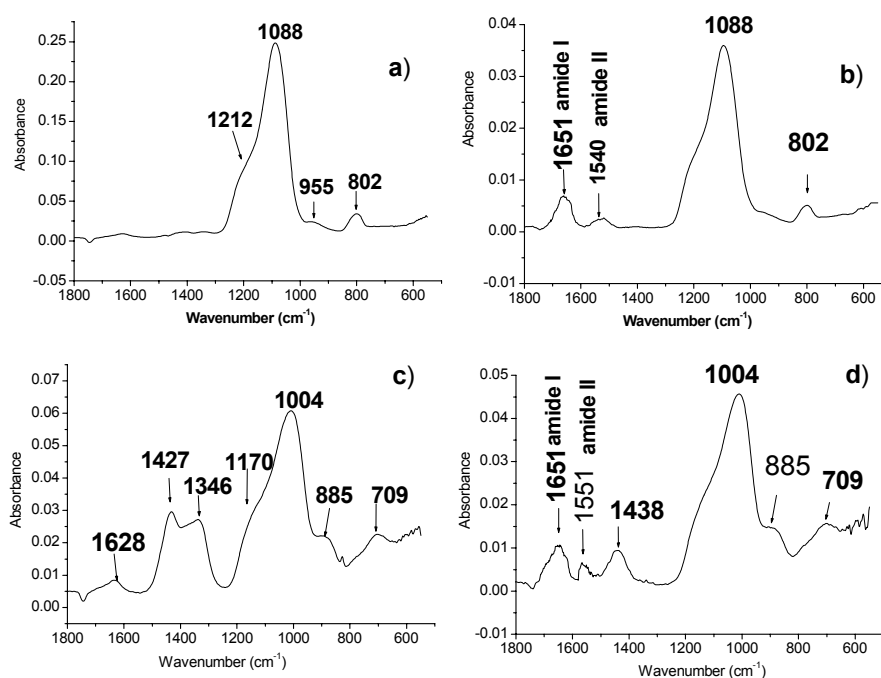


Fig. 5. ATR FTIR spectra of aluminosilicate prepared with silicic acid before (a) and after 24 h incubation in fibrinogen buffer solution (b) and the corresponding spectra of the sample prepared with TEOS (c, d) in the same conditions.

The dominant band in these figures is the stretching vibration of Si-O-Si and Al-O-Al bonds at around 1888 and 1004  $\text{cm}^{-1}$  respectively for the two samples. In the case of the sample with silicic acid, the intensity of this band is drastically reduced upon incubation, as well as the band at 802  $\text{cm}^{-1}$  assigned to  $\text{AlO}_4$  units. The corresponding bands for the TEOS-related sample are only slightly reduced, but the band intensity around 1427  $\text{cm}^{-1}$  decreases significantly upon incubation, indicating the dissolution of nitrates species. Fibrinogen adsorption is evidenced by the amide I (around 1651  $\text{cm}^{-1}$ ) and amide II (1538–1550  $\text{cm}^{-1}$ ) bands which are

shifted towards higher wave number upon adsorption (compared with the amide bands of the native protein). Deconvolution of amide I region was performed for both spectra in Fig. 5b, d assuming a Gaussian profile and the resultant spectra were smoothed with a 9-point Savitsky-Golay smooth function to remove the noise. Generally, the bands between 1618–1625  $\text{cm}^{-1}$ , 1630–1640, 1645–1655, 1660–1670 and around 1685  $\text{cm}^{-1}$  are related to  $\beta$  sheet-intermolecular (aggregates),  $\beta$  sheet-native,  $\alpha$  helix and turns conformation respectively [11, 12]. The curve fitting procedure was employed in order to evaluate quantitatively the secondary structure of the fibrinogen adsorbed on both materials, and the percentage of each secondary structure was calculated from the corresponding band areas [5]. Fig. 6 shows the deconvolution of amide I band of native fibrinogen (a) and adsorbed on the different aluminosilicates samples (b, c). Significant differences were observed for  $\alpha$  helix, turns and  $\beta$  sheet contributions, as revealed in Figure 7. According to literature [10], a lower sheet/turn ratio appears to indicate inferior biocompatibility. On this basis, the samples prepared with silicic acid seem to have a superior biocompatibility. Other studies [3, 9] reported that fibrinogen adsorbs in general more strongly to hydrophobic surfaces than to hydrophilic ones. In Figure 5, the intensity of the amide bands indicates that aluminosilicates sample prepared with silicic acid is favorable to fibrinogen adsorption.

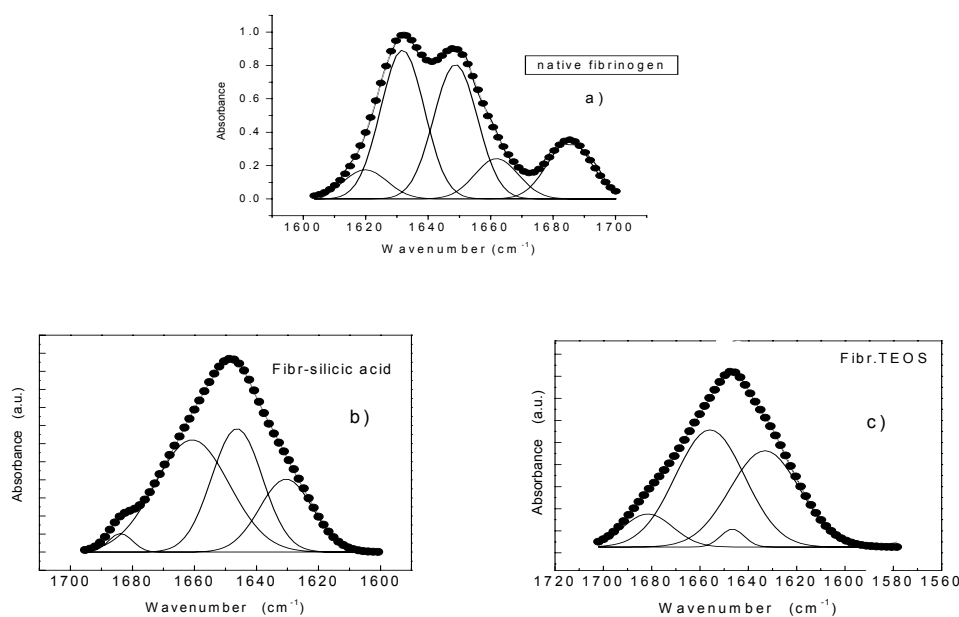


Fig. 6. Deconvolution of amide I band of native fibrinogen (a) and adsorbed on aluminosilicates sample with silicic acid (b) and TEOS respectively (c).

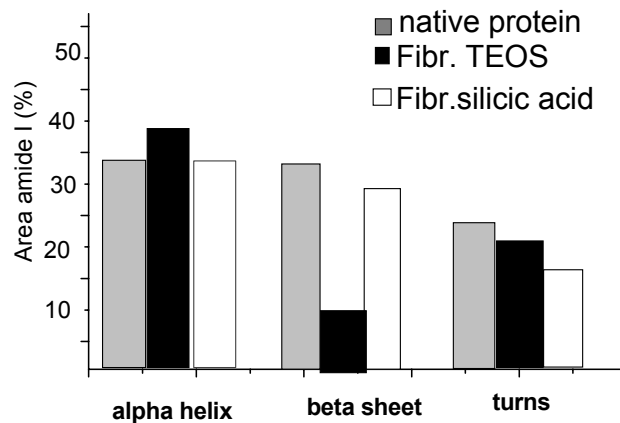


Fig. 7. Distribution of secondary structure in fibrinogen.

## CONCLUSIONS

Two different aluminosilicates bioglass matrices are prepared by sol-gel route and characterized using FTIR spectroscopy. The infrared functional groups were identified to be  $\text{SiO}_4$  and  $\text{AlO}_4$  units. Thermal treatment reveals the almost complete disappearance of the band typical to nitrogen species around  $1400\text{ cm}^{-1}$ , for both samples. Similar results are obtained also for the samples prepared with TEOS. The biocompatibility of the samples was evaluated with respect to fibrinogen adsorption using ATR FTIR technique. Deconvolution of amide I band of fibrinogen upon adsorption indicates that aluminosilicates prepared with silicic acid as starting material exhibit a superior biocompatibility compared with that of the sample obtained with TEOS.

*Acknowledgements.* This work was partially supported by Grant MATNANTECH-CEEX no. 100/2006.

## REFERENCES

1. CAVALU, S., S. CÎNTA PÎNZARU, N. PEICA, G. DAMIAN, W. KIEFER, Hyaluronidase adsorption onto silver nanoparticles, *J. Optoelectronics Adv. Mater.*, 2007, **9**, 3,683–693.
2. CAVALU, S., On the conformation and stability of pharmaceutical protein formulations by complementary spin label and Fourier deconvolution techniques, *Asian J. Physics*, 2006, **15** (2), 141–147.
3. DONG, A., W.S. CAUGHEY, Infrared methods for study of hemoglobin reaction and structures, *Methods Enzymol.*, 1994, **232**, 139–175.

4. DONG, A., J.D. MAYER, J.L. BROWN, M.C. MANNING, J.F. CARPENTER, Comparative Fourier transform infrared and circular dichroism spectroscopic analysis of  $\alpha(1)$ -proteinase inhibitor and ovalbumin in aqueous solution, *Arch. Biochem. Biophys.*, 2000, **383**, 148.
5. DAMIAN, G., S. CAVALU, Comparative study of amide I and III bands of ovalbumin and bovine serum albumin by FTIR spectroscopy, *Asian Chem. Lett.*, 2005, **9**, 1&2, 3–7.
6. GREEN, R.J., I. HOPKINSON, R.A.L. JONES, Unfolding and intermolecular association in globular proteins adsorbed at interfaces, *Langmuir*, 1999, **15**, 5102–5110.
7. HAYNES, C.A., W. NORDE, Globular proteins at solid/liquid interfaces, *Colloids Surf. B*, 1994, **2**, 517–566.
8. NAKAMOTO, K., *Infrared Spectra of Inorganic and Coordination Compounds*, John Wiley & Sons Inc., New York-London, 1963.
9. SAGVOLDEN G., I. GIAVER, J. FEDER, Characteristic protein adhesion forces on polystyrene substrates by AFM, *Langmuir*, 1998, **14**, 5984–5987.
10. SIMON, V., D. ENIU, A. GRITCO, S. SIMON, Thermal and spectroscopic investigation of sol-gel derived aluminosilicate bioglass matrices, *Proceedings of International Conference on Biomaterials & Medical Devices – BIOMMEDD*, 2007, Iași, p. 252.
11. TUNC, S., M.F. MAINZ, G. STEINER, L. VAZQUEZ, M.T. PHAM, R. SALZER, *In situ* conformational analysis of fibrinogen adsorbed on Si surfaces, *Colloids and Surfaces B: Biointerfaces*, 2005, **42**, 219–225.
12. VELMETTE, P., V. GAVREAU, M. PEZOLET, G. LAROCHE, Albumin and fibrinogen adsorption onto phosphatidylcholine monolayers investigated by Fourier transform infrared spectroscopy, *Colloids and Surface B: Biointerfaces*, 2003, **29**, 285–295.

